Cell Reports

Placenta Colonization by Fusobacterium nucleatum is mediated by binding of the Fap2 lectin to placenta displayed Gal-GalNAc

--Manuscript Draft--

Manuscript Number:	CELL-REPORTS-D-20-04881
Full Title:	Placenta Colonization by Fusobacterium nucleatum is mediated by binding of the Fap2 lectin to placenta displayed Gal-GalNAc
Article Type:	Research Article
Keywords:	Fusobacterium nucleatum; Adverse pregnancy outcomes; Gal-GalNAc; Placenta
Order of Authors:	Lishay Parhi
	Jawad Abed
	Amjad Shhadeh
	Tamar Alon
	Shiran Udi
	Joseph Tam
	Debra Goldman-Wohl
	Simcha Yagel
	Ofer Mandelboim
	Gilad Bachrach, Ph.D.
Abstract:	While the existence of an indigenous placenta microbiota remains controversial, several pathogens are known to be involved in adverse pregnancy outcomes. Fusobacterium nucleatum is an oral bacteria associated with preterm birth. Oral fusobacteria translocate to the placenta hematogenously, however the mechanisms localizing them to the placenta remain unclear. Here we demonstrate that the level of Gal-GalNAc found on trophoblasts facing entering maternal blood rises along gestation and is recognized by the fusobacterial Fap2 Gal-GalNAc lectin. F. nucleatum binding to human and mouse placenta correlates with Gal-GalNAc levels and is reduced upon O-glycanase treatment or with soluble Gal-GalNAc. Fap2-inactivated F. nucleatum show reduced binding to Gal-GalNAc-displaying placental sections. In a mouse model, intravenously injected Fap2-expressing F. nucleatum but not a Fap2 mutant, reduces mouse fetal survival by 75%. Fetal death by Fap2 expressing fusobacteria is prevented with antibiotic treatment, suggesting prophylaxis might be beneficial when performing dental surgery during pregnancy.

Highlights

- **Gal-GalNAc levels rises along gestation in human and mouse placenta**
- **Placental Gal-GalNAc is displayed on trophoblasts in direct contact with entering maternal blood**
- **The Fap2 Gal-GalNAc lectin mediates *F. nucleatum* binding to Gal-GalNAc over-displayed in the placenta**
- **Blood-borne Fap2-expressing *F. nucleatum* localizes to mouse placenta inducing fetal death that can be prevented with metronidazole**

Placenta Colonization by *Fusobacterium nucleatum* is mediated by binding of the Fap2 lectin to placenta displayed Gal-GalNAc

Lishay Parhi[1], Jawad Abed[1], Amjad Shhadeh[1], Tamar Alon[1], Shiran Udi[2], Joseph Tam[2], Debra Goldman-Wohl[3], Simcha Yagel[3], Ofer Mandelboim[4#], Gilad Bachrach[1#].

1. The Institute of Dental Sciences, The Hebrew University-Hadassah School of Dental Medicine, Jerusalem, Israel
2. Obesity and Metabolism Laboratory, The Institute for Drug Research, School of Pharmacy, Faculty of Medicine, The Hebrew University of Jerusalem, Jerusalem, Israel
3. Magda and Richard Hoffman Center for Human Placenta Research, Department of Obstetrics and Gynecology, Hebrew University Hadassah Medical Center, Jerusalem, Israel
4. Department of Immunology and Cancer Research, Institute for Medical Research Israel Canada (IMRIC), Hebrew University-Hadassah Medical School, Jerusalem, Israel

[#] These authors contributed equally to this work

Correspondence: oferm@ekmd.huji.ac.il (O.M.), giladba@ekmd.huji.ac.il (G.B.)

Summary

While the existence of an indigenous placenta microbiota remains controversial, several pathogens are known to be involved in adverse pregnancy outcomes. *Fusobacterium nucleatum* is an oral bacteria associated with preterm birth. Oral fusobacteria translocate to the placenta hematogenously, however the mechanisms localizing them to the placenta remain unclear. Here we demonstrate that the level of Gal-GalNAc found on trophoblasts facing entering maternal blood rises along gestation and is recognized by the fusobacterial Fap2 Gal-GalNAc lectin. *F. nucleatum* binding to human and mouse placenta correlates with Gal-GalNAc levels and is reduced upon O-glycanase treatment or with soluble Gal-GalNAc. Fap2-inactivated *F. nucleatum* show reduced binding to Gal-GalNAc-displaying placental sections. In a mouse model, intravenously injected Fap2-expressing *F. nucleatum* but not a Fap2 mutant, reduces mouse fetal survival by 75%. Fetal death by Fap2 expressing fusobacteria is prevented with antibiotic treatment, suggesting prophylaxis might be beneficial when performing dental surgery during pregnancy.

Introduction

The sterile womb hypothesis was the prevailing paradigm in obstetrics until recently. Implementation of recent omics approaches sparked an ongoing controversy regarding the existence of a placenta microbiome and of its possible role in normal pregnancy (Aagaard et al., 2014; Aagaard, 2020; de Goffau et al., 2019; Dudley, 2020; Gschwind et al., 2020; Theis et al., 2020). Unlike the case in normal pregnancy, in utero infection as a risk for pregnancy has been known for ages (de Goffau et al., 2019; Goldenberg et al., 2010; Hill, 1998; Naeye and Peters, 1978; Villamor-Martinez et al., 2020; Watts et al., 1992).

Preterm birth is birth before 37 weeks of gestation. It is estimated that 15 million babies are born preterm annually worldwide (World-Health-Organization, 2018). Complications due to preterm birth are the leading cause of death among children under 5 years of age and many survivors face lifetime disabilities (Liu et al., 2012). Microbiological studies suggested that intrauterine infection might account for 25–40% of preterm births (Goldenberg et al., 2000).

During pregnancy, sex hormones such as estrogen and progesterone are elevated. This alters the periodontal tissue response to microbial plaque, thus indirectly contributing to periodontal diseases (Bobetsis et al., 2020; Gursoy et al., 2013; Loe and Silness, 1963). Gingival inflammation accompanied with gingival bleeding facilitates entry of oral bacteria to the circulatory system and increases the frequency of transient bacteremia by oral bacteria (Figuero et al., 2020). Accordingly, *Fusobacterium nucleatum* a bacterial species associated with development of periodontitis, is among the most prevalent bacteria found in adverse pregnant outcome including intra-amniotic infection, stillbirth, neonatal sepsis, hypertensive disorders of pregnancy and preterm births (Han et al., 2010; Han et al., 2009; Hill, 1993, 1998) (for review see (Vander Haar et al., 2018)).

Fusobacterium nucleatum is an oral, gram negative, anaerobic, nonmotile, rod-shaped bacteria (Moore and Moore, 1994; Sanders et al., 2018; Socransky et al., 1998), that can function as an invasive (Han et al., 2000), adherent (Weiss et al., 2000), pro-inflammatory pathogen (Han et al., 2000). It is among the pathobionts that outgrow during dysbiosis preceding periodontal disease (Nozawa et al., 2020; Socransky et al., 1998). Numbers of *F. nucleatum* rise 10,000 fold (Socransky et al., 1998) during the development of gingivitis that precedes periodontal disease (Nozawa et al., 2020) potentially increasing the probability of their hematogenous spread.

The frequency of *F. nucleatum* infection in amniotic fluid was approximately 10-30% in women with preterm labor with intact membranes and 10% in women with premature rupture of membranes (Han et al., 2009; Hill, 1993, 1998; Watts et al., 1992). In a case of term stillbirth, *F. nucleatum* was isolated as a pure culture from the lung and stomach of the stillborn infant. An identical clone was found in the mother's subgingival plaque, while no fusobacteria was detected in her vaginal and rectal floras (Figuero et al., 2020; Han et al., 2010). The causative role of *F. nucleatum* in pregnancy complications has been demonstrated in a mouse model. Oral *F. nucleatum* isolates injected into the tail vein (simulating transient bacteremia) of pregnant mice specifically colonized the murine placenta. In the mouse placenta, *F. nucleatum* infected the decidua basalis (Han et al., 2004). Placenta colonization was species specific as a control organism inoculated similarly could not be detected in the placenta (Han et al., 2004). Once colonized in the

placenta, *F. nucleatum* spread to the amniotic fluid, the fetal membranes and the fetus (Han et al., 2004), inducing TLR4 dependent inflammatory response accompanied by neutrophil infiltration that resulted in preterm deliveries and stillbirths (Liu et al., 2007).

The decidua basalis of the placenta (where fusobacterial colonization initiates), is an area characterized by large venous sinuses. It was therefore speculated that the slow blood flow rate and consequent low shear forces in the venous sinuses provide an opportunity for the *Fusobacterium nucleatum* Adehesin A (FadA) of hematogenous *F. nucleatum* to adhere to vasculature endothelial cadherin (VE-cadherin) on endothelial cells and invade them (Han et al., 2004; Ikegami et al., 2009). Binding of FadA VE-cadherin also causes VE-cadherin to migrate away from the cell-cell junction thus increasing the endothelial permeability and allowing *F. nucleatum* placenta penetration (Vander Haar et al., 2018). Indeed, a FadA-inactivated *F. nucleatum* mutant was found severely deficient in colonizing murine placenta (Ikegami et al., 2009). However, although VE-cadherin is expressed on cytotrophoblasts (Zhou et al., 1997), is not it is not clear whether it is overexpressed in the placenta, and placenta reduced blood shear rate by its own, could not fully explain *F. nucleatum* species tropism to the placenta.

F. nucleatum is remarkable for its extensive ability to attach to a large variety of oral bacterial species and to various host cells. Many of these attachments are inhibited by galactose. Transposon mutagenesis identified the Fap2 outer membrane protein (previously associated with apoptosis induction (Kaplan et al., 2005; Kaplan et al., 2010)) as the fusobacterial galactose binding lectin (Coppenhagen-Glazer et al., 2015). Fap2-deficient *F. nucleatum* mutants were impaired in attachment to the periopathogen *P. gingivalis,* to erythrocytes and to human embryonic kidney cells (HEK 293T). Fap2-deficient *F. nucleatum* mutants were also impaired in placenta colonization compared to the isogenic *F. nucleatum* ATCC 23726 parent species (Coppenhagen-Glazer et al., 2015).

Further characterization of Fap2 revealed that it selectively attaches to Gal-GalNAc. Gal-GalNAc belongs to a family of antigens found to be over-displayed in certain tumors (Abed et al., 2016; Abed et al., 2017; Springer et al., 1975) and during fetal development (Barr et al., 1989; Jeschke et al., 2007; Richter et al., 2000). Such antigens are known as oncofetal antigens.

Herein, we studied the role of Fap2 in the specific translocation of fusobacteria to the placenta. We found that Gal-GalNAc is displayed in the placenta intervillous spaces where it is exposed to the entering maternal blood. Gal-GalNAc level increases in the placenta along the gestational age in both the human and murine placenta. This increased Gal-GalNAc level facilitates Fap2 binding, and attachment of fusobacteria to sections prepared from human and mice placenta. Moreover, IV-injected Fusobacteria were found in the placenta of pregnant mice if inoculation was performed at late pregnancy compared to early pregnancy when placenta Gal-GalNAc levels are low. Fusobacterial accumulation in mouse placenta at late gestational age was Fap2 dependent. As demonstrated previously (Han et al., 2004; Ikegami et al., 2009), fusobacterial colonization in the murine fetoplacental unit resulted in fetal death. Importantly, antibiotic administration prevented fetal death. As dental treatment might increase the probability of fusobacterial transient bacteremia, our results suggest that prophylactic treatment for pregnant women undergoing dental surgery might be considered, as is the case in treatment of additional risk groups.

Results

Gal-GalNAc display increases along pregnancy progression in human and mouse placenta.

Binding of *F. nucleatum* to many bacterial and mammalian cells can be inhibited with sugars containing D-galactose (Bachrach et al., 2005; Kolenbrander and London, 1993). We previously identified the outer membrane protein Fap2 as the lectin that binds galactose moieties and mediates cell binding by *F. nucleatum* (Coppenhagen-Glazer et al., 2015). Fap2 - deficient fusobacterial mutants were found to be impaired in attaching to various mammalian cells and in placenta colonization (Coppenhagen-Glazer et al., 2015). We later found that Fap2 preferentially binds Gal-GalNAc (Abed et al., 2016).

Gal-GalNAc is over displayed in colorectal and breast cancers (Abed et al., 2016; Parhi et al., 2020; Yang and Shamsuddin, 1996), and its attachment by Fap2 enables specific colonization and enrichment of *F. nucleatum* in both cancers (Abed et al., 2016; Parhi et al., 2020). Gal-GalNAc has also been previously detected in the placenta (Jeschke et al., 2002; Richter et al., 2000).

These observations led to our hypothesis that Gal-GalNAc display in the placenta may facilitate attachment and colonization of the placenta by blood-borne fusobacteria. To test this hypothesis, we first measured the level of Gal-GalNAc in the human placenta during pregnancy. For this, we used a human placenta Tissue Microarray (TMA) with sections collected at different gestational age. We assessed Gal-GalNAc level using fluorescein isothiocyanate (FITC)-labeled peanut agglutinin (PNA), a Gal-GalNAc [Gal – β(1/3)GalNAc] specific lectin. As is shown in Figure 1A, Gal-GalNAc level increases significantly along the progression of human pregnancy ($p < 0.0001$). Next, we tested whether Gal-GalNAc level changes in the placenta due to placenta pathologies. We did not detect alterations in Gal-GalNAc levels between samples from placenta of preterm (all over 26 weeks of pregnancy), preeclampsia, and intrauterine growth restriction pregnancies, compared to those from normal pregnancies (Figure 1B). With the restriction of our relative small sample pool, our results indicate that placental Gal-GalNAc levels are independent of the tested placenta pathologies.

To test the relevance of using a murine model for studying the role of Gal-GalNAc in placenta colonization by fusobacteria, we first tested whether similar to humans, Gal-GalNAc level rises in the mouse placenta along pregnancy progression. For this purpose, we created a mouse placenta TMA containing sections collected along E11.5 to E18.5 days post gestation (Supplementary Figure 1). We found, that in accordance with the human placenta, Gal-GalNAc level in the mouse placenta increase significantly with gestation age ($p < 0.0001$, Figure 1C).

Fusobacteria attach to Gal-GalNAc displayed by placenta cells.

To determine whether Gal-GalNAc displayed in the mouse placenta directs fusobacterial colonization, we tested whether fusobacteria attach preferentially to Gal-GalNAc displaying cells. Fluorescence microscopy analysis of mouse placenta samples demonstrated that Cy5-labeled *F. nucleatum* ATCC 23726 preferentially attach (3.6 fold increase, $p = 0.0039$) to placenta cells that display Gal-GalNAc (Figure 2A).

Next, we tested whether GalNAc can inhibit binding of fluorescently-labeled fusobacteria to placenta samples in the mouse placenta TMA. Indeed, GalNAc reduced

attachment of *F. nucleatum* ATCC 23726 to the placenta samples by 2.2 fold ($p < 0000.1$, Figure 2B).

We then tested whether placenta-displayed Gal-GalNAc can be removed by O-glycanase, an enzyme that cleaves GalNAc from serine or threonine residues of glycoproteins. As expected, O-glycanase reduced staining of placenta-TMA with FITC-PNA by 2.8 fold ($p = 0.0007$, Figure 2C). Accordingly, O-glycanase treatment reduced binding of *F. nucleatum* ATCC 23726 to the mouse placenta samples by 5.3 fold ($p = 0.046$, Figure 2D). These data support our hypothesis that placenta-displayed Gal-GalNAc play an important role in *F. nucleatum* placenta enrichment and localization.

Fap2 mediates fusobacterial attachment to Gal-GalNAc displayed by the placenta.

We recently identified the fusobacterial outer-membrane protein Fap2 to function as the Gal-GalNAc fusobacterial binding lectin (Abed et al., 2016). In order to determine the role of Fap2 in fusobacterial attachment to the placenta we compared binding of fluorescently-labeled Fap2-expressing *F. nucleatum* ATCC 23726 and of its Fap2-deficient isogenic mutants K50 and D22 (Coppenhagen-Glazer et al., 2015) to human and mouse placental TMAs. Before competing for binding to placenta tissue, we confirmed the Fap2-dependent Gal-GalNAc -binding function in the ATCC 23726 (and lack of it in K50 and D22) using a GalNAc inhabitable hemagglutination assay (Coppenhagen-Glazer et al., 2015)(Figure 3A).

While binding of the tested Fap2-inactivated mutant K50 to first trimester human placenta samples, was similar to that of wild-type *F. nucleatum* ATCC 23726, K50 displayed significant impaired ($p < 0.0001$) attachment to 2nd and 3rd trimester human placenta sections compared with the wild-type *F. nucleatum* ATCC 23726 (Figure 3B). Accordingly, the Fap2-inactivated mutants K50 and D22 displayed significant impaired attachment to mouse placenta sections compared with the wild-type *F. nucleatum* ATCC 23726 ($p < 0.0001$) (Figure 3 C-D). We also saw preferential co-localization of wild-type *F. nucleatum* ATCC 23726 with mouse placenta cells displaying Gal-GalNAc compared to the K50 Fap2-inactivated mutant (78.1% versus 23.6%, $p < 0.0001$, Figure 3E) strengthening our hypothesis that Fap2 mediates fusobacterial binding to Gal-GalNAc displayed on placenta cells.

Flow cytometry (experimental scheme presented in Figure 4A) reveled that attachment of *F. nucleatum* ATCC 23726 to placenta cells prepared from mice at day E12.5 of gestation was significantly lower ($p = 0.046$) than attachment to cells prepared from placenta at day E17.5 (Figure 4B). This result is in agreement with our finding that Gal-GalNAc level increases along the progression of mouse pregnancy (Figure 1C). Attachment of the Fap2-inactivated mutant D22 to the placenta cells was weaker than that of the Fap2 expressing ATCC 23726 parent, and was not enhanced with placenta gestational age (Figure 4B). Interestingly, attachment of *F. nucleatum* ATCC 23726 to blood vessels leading to the mouse placenta also increased with pregnancy progression ($p = 0.046$), and again, was higher than that of the D22 Fap2-mutant, whose binding to cells of blood vessels leading to the placenta was not influence by the gestation age (Figure 4C). These results suggest that Gal-GalNAc level in the blood vessels leading to the placenta, rises along the pregnancy in parallel to the Gal-GalNAc level in the placenta. Increased Gal-GalNAc level in the blood vessels entering the placenta, can greatly facilitate placenta-colonization by hematogenous fusobacteria.

Fap2 Mediates placenta colonization by blood-borne *F. nucleatum* in BALB/c mice

Transient bacteremia with oral microbes during daily oral hygiene and during dental treatment is common (Dayer et al., 2015; Lockhart et al., 2008), even more-so during pregnancy (Figuero et al., 2020; Offenbacher et al., 1996) and therefore enables access of oral fusobacteria to the circulatory system. Fusobacteria inoculated IV (simulating transient bacteremia) into BALB/c mice, were previously shown to localize in the placenta (Han et al., 2004). We therefore, used the BALB/c mouse model to investigate the role of Gal-GalNAc and of Fap2 in the ability of fusobacteria to colonize the placenta *in vivo*. Co-challenge with ATCC 23726 and the K50 Fap2-inactivated mutant co-injected IV into pregnant BALB/c mice, demonstrated the involvement of Fap2 and Gal-GalNAc -dependent placenta colonization by *F. nucleatum* ATCC 23726. BALB/c mice were co-challenged with a mixture of ATCC 23726 and K50 at days E12.5, E15.5 or E17.5 of gestation by tail vein intravascular injection. 24 hours post infection, placentas were

harvested and fusobacteria quantified using qPCR. At day 12.5 of gestation, when we found placenta Gal-GalNAc level to be low (Figure 1C), placenta localization of ATCC 23726 and K50 was similar (Figure 4D). However, co-challenge with ATCC 23726 and K50 mixed together on day 15.5 and 17.5 of gestation, when we found that placenta Gal-GalNAc level is significantly higher than that at day 12.5 ($p = 0.0079$, Figure 1C), resulted in a clear enrichment of ATCC 23726 in the placenta (mean of competition index 6, $p = 0.0156$ and 3.4, $p = 0.0317$ respectively; Figure 4D).

The fact that both K50 and ATCC 23726 colonized the placenta in a similar manner at day 12.5 of gestation (when placenta Gal-GalNAc levels are low), indicates that in addition to Fap2- Gal-GalNAc interactions, fusobacteria utilize co-factors mechanisms to colonize the placenta. These may include the hydrodynamic properties such as reduced pressure and flow rate of the sinus entering the placenta (Han et al., 2004), as well as additional host-recognizing receptors including FadA (Ikegami et al., 2009).

Gal-GalNAc is displayed to the maternal blood entering the human placenta

Immunofluorescence microscopy analysis of human placenta TMAs revealed that Gal-GalNAc is mainly displayed on trophoblasts (Figure 5 A-B). Placental trophoblasts include syncytiotrophoblast and cytotrophoblasts and provide structural and biochemical barriers between the maternal and fetal compartments during pregnancy (Figure 5C). They also serve as an important endocrine organ that produces numerous growth factors and hormones that support and regulate the development and growth of the placenta and fetus (Wang and Zhao, 2010).

The syncytiotrophoblast covers the entire surface of fetal villous surface and is in direct contact with maternal blood (Figure 5 A, C). It transport nutrients and remove waste products to promote fetal growth. Cytotrophoblasts are considered to be stem cells for syncytiotrophoblast and form a layer under the syncytiotrophoblast (Figure 5 A). We did not observe differences in the level of Gal-GalNAc displayed by cytotrophoblasts and by the syncytiotrophoblast (Figure 5A). Importantly, in agreement with our initial human

placenta Gal-GalNAc screen (Figure 1A), we saw an increase of the Gal-GalNAc level in the trophoblasts along pregnancy progression (Figure 5B).

The placenta is a unique vascular organ that incorporates blood circulating from both the maternal and the fetal systems and thus has two separate blood circulatory systems: (1) the maternal-placental (uteroplacental) blood circulation (illustrated in dark red in Figure 5), and (2) the fetal-placental (fetoplacental) blood circulation (illustrated in dark sand-color in Figure 5). The uteroplacental circulation begins with the maternal blood flow into the intervillous space through decidual spiral arteries. Exchange of oxygen and nutrients take place as the maternal blood flows around fetal villi in the intervillous space. The trophoblasts, (syncytiotrophoblast in particular) are the exterior cells of the fetal villi that interact with the maternal blood. Our observation that the villi's trophoblasts display high levels of Gal-GalNAc provides a new mechanism by which blood-borne *F. nucleatum* entering from the maternal blood flow is exposed to Gal-GalNAc, attaches to it and colonize the placenta (illustrated in Figure 5C).

Antibiotic prophylaxis prevents fetal death by fusobacteria in the mouse model

Administration of antibiotic prophylaxis before invasive dental procedures for prevention of infective endocarditis (IE) has been practiced for over 50 years (Thornhill et al., 2018). As bacteremic oral fusobacteria are a risk factor for abnormal pregnancy outcomes, we wanted to estimate the possible benefit in antibiotic prophylaxis for pregnant women. For this purpose, we used the mouse pregnancy model as illustrated in the schematic representation in Figure 6A. Mice at day 15.5 of gestation were sham treated with PBS vehicle, or IV inoculated with *F. nucleatum* ATCC 23726 or with K50. A sub-group of the mice inoculated with *F. nucleatum* ATCC 23726 were treated with metronidazole 30 minutes pre-inoculation, and 8h, 24h and 48h post inoculation. 72h post inoculation fetal viability and placenta parameters were measured. Inoculation with the fap2-defective K50 strain did not affect fetal viability in a statistical significant manner. However, inoculation with the Fap2-expressing *F. nucleatum* ATCC 23726 parent strain, reduced fetal viability by 30% ($p < 0.0001$). Importantly, metronidazole treatment prevented fetal death by the inoculated *F. nucleatum* ATCC 23726 (Figure 6B). Inoculation

with both *F. nucleatum* ATCC 23726 and K50 resulted in a significant reduction in fetal weight and length. Demonstrating again the ability (though reduced) of *F. nucleatum* to colonize the placenta in the absence of Fap2. While the deleterious effect of *F. nucleatum* ATCC 23726 on fetus weight was prevented with antibiotic treatment, reduction in fetal length was not. Infection with *F. nucleatum* ATCC 23726 had no effect on placenta weight or diameter under the tested conditions (Figure 6 C-F).

Discussion

While oral fusobacteria are found in samples from abnormal pregnancy outcomes (Han et al., 2009; Hill, 1993, 1998; Vander Haar et al., 2018), the mechanisms by which fusobacteria specifically home and localize to the placenta have not been fully explored. Increased blood flow, slow blood flow rate (due to conversion of the spiral arteries) and consequent reduced haemodynamic sheer forces in the venous sinuses (Han et al., 2004), hypoxia and placenta-induced immune-privileged microenvironment are factors that undoubtedly contribute for fusobacterial colonization and survival (Vander Haar et al., 2018). However, these local microenvironmental conditions were not sufficient to enable localization of a control organism in the placenta (Han et al., 2004). Therefore, it seems that specific factors and mechanisms are required for placenta colonization by fusobacteria. Herein, using human samples and a mouse pregnancy model, we found that the placenta displays specific glycans that mediate fusobacterial enrichment in the placenta.

Our experiments support that fusobacterial Fap2 and host Gal-GalNAc, are involved in fusobacterial placenta localization and enrichment. Interestingly, Fap2 – dependent fusobacterial attachment was observed not only in the placenta, but also in the blood vessels leading to the placenta, suggesting that increased Gal-GalNAc display is coordinated both in fetal and maternal tissues. This might suggest a chemo-attraction mechanism in which drift of blood-born fusobacteria is slowed in the entrance to the placenta due to increased Gal-GalNAc level displayed on the inner wall of the blood vessels perhaps similar to the rolling of leukocyte during leukocyte extravasation. After being slowed, the fusobacteria enter intervillous spaces where high amounts of Gal-GalNAc displayed by trophoblasts allow sufficient Fap2- Gal-GalNAc interactions to bind the bacteria and form tight

adhesions. Next, FadA – VE-cadherin interactions may increase the endothelial permeability to enable the bacteria to cross the trophoblast layer and transmigrate to the fetal blood vessels in a mechanism suggested previously (Vander Haar et al., 2018).

Interestingly, Fap2 shown here to mediate placenta colonization by fusobacteria, also activates the human (but not mouse) TIGIT killing-suppressing receptor expressed on T cells and natural killer (NK) cells (Gur et al., 2015). NK cells play an important role in promotion of normal human pregnancy (El Costa et al., 2009; Gamliel et al., 2018). Decidual NK cells comprise 50%–70% of decidual lymphocytes during the first trimester (Koopman et al., 2003), a pregnancy stage where Gal-GalNAc levels are low and accordingly the probability of placental colonization by fusobacteria. Future humanized mice might enable better understanding of the effect of fusobacteria - NK cells interactions in pregnancy.

Trophoblasts and cancer share obvious phenotypic features such as highly proliferating cells, the ability to invade adjacent tissue, and promoting angiogenesis (Seiler et al., 2017) (Holtan et al., 2009). This similarity is also manifested with common antigens, oncofetal antigens that are hypothesized to facilitate progression of both circumstances. Gal-GalNAc has been known previously to constitute such an oncofetal antigen. Interestingly, Fap2 – expressing *F. nucleatum* that targets Gal-GalNAc is found in both cellular niches.

Plasmodium falciparum the cause of malaria is also found in both the placenta and in tumors. VAR2CSA is the protein hypothesized to guide malaria colonization in the placenta and in tumors by attaching to chondroitin sulfate glycosaminoglycan modification to proteoglycans. Chondroitin sulfate is an oncofetal antigen shared between placental trophoblasts and cancer cells (Agerbaek et al., 2019; Ayres Pereira et al., 2016). Recombinant VAR2CSA to target oncofetal chondroitin sulfate shows promise for novel cancer diagnostics and therapeutics (Agerbaek et al., 2019; Salanti et al., 2015) and for generating a combinatorial Human Papillomavirus and placental malaria vaccine (Janitzek et al., 2019). The parallel roles played by VAR2CSA - chondroitin sulfate and Fap2 and Gal-GalNAc are intriguing and require farther investigation.

Lastly, our results also show that antibiotic treatment prevented fetal death by inoculated fusobacteria. Administration of antibiotic prophylaxis in invasive dental procedures for prevention of infective endocarditis (IE) has been practiced for over 50 years and remains the global standard of care for patients at risk (Dayer et al., 2015; Thornhill et al., 2018). Transient bacteremia is common during dental treatment especially during periodontal surgery. However, it is estimated that frequency of bacteremia from routine daily activities is far greater than that resulting from dental treatment (For review see (Wilson et al., 2008)). This conclusion lead to a decision in both the United States and Europe in 2007 to cease antibiotic prophylaxis for patients at moderate risk for IE (Dayer et al., 2015). In 2008, in the United Kingdom, guidelines were amended to cease such antibiotic prophylaxis completely which correlated with a significant increase in the incidence of IE (Dayer et al., 2015). To date, most evidence indicate that nonsurgical periodontal therapy during the second trimester of gestation does not affect pregnancy outcomes (for review see (Bobetsis et al., 2020)). However, our results here suggest that similar to prophylaxis practiced for high risk IE patients, prophylaxis (or postponing non-urgent dental treatment) might be considered with pregnant women at high risk.

Author Contributions

L.P., S.Y., D.G.W., O.M., and G.B., conceived of the research idea, designed experiments, and wrote the article. D.G.W., and S.Y., helped interpret clinical data for this article. L.P. designed and performed *in vitro* and *in vivo* experiments. J.A., A.S., T.A., S.A., helped perform *in vitro* and *in vivo* experiments. J.T., helped create critical reagents.

Acknowledgments

The authors thank the donors, the RCWIH BioBank, the Lunenfeld-Tanenbaum Research Institute, and the Mount Sinai Hospital/UHN Department of Obstetrics & Gynecology for the human specimens used in this study (http://biobank.lunenfeld.ca). Professor Norman Grover for his valuable assistance in statistics, Dr. Zakhariya Manevitch and Dr. Yael

Feinstein-Rotkopf for their valuable help in microcopy, Noam Koren and Dr. Oded Heyman for their valuable discussion. This work was supported by the Israel Cancer Research Fund Project grant, the Israel Science Foundation Moked grant and the Israel Ministry of Science and Technology Personalized Medicine grant.

Declaration of Interests

The authors declare no competing interests

Figure & legends

Figure 1

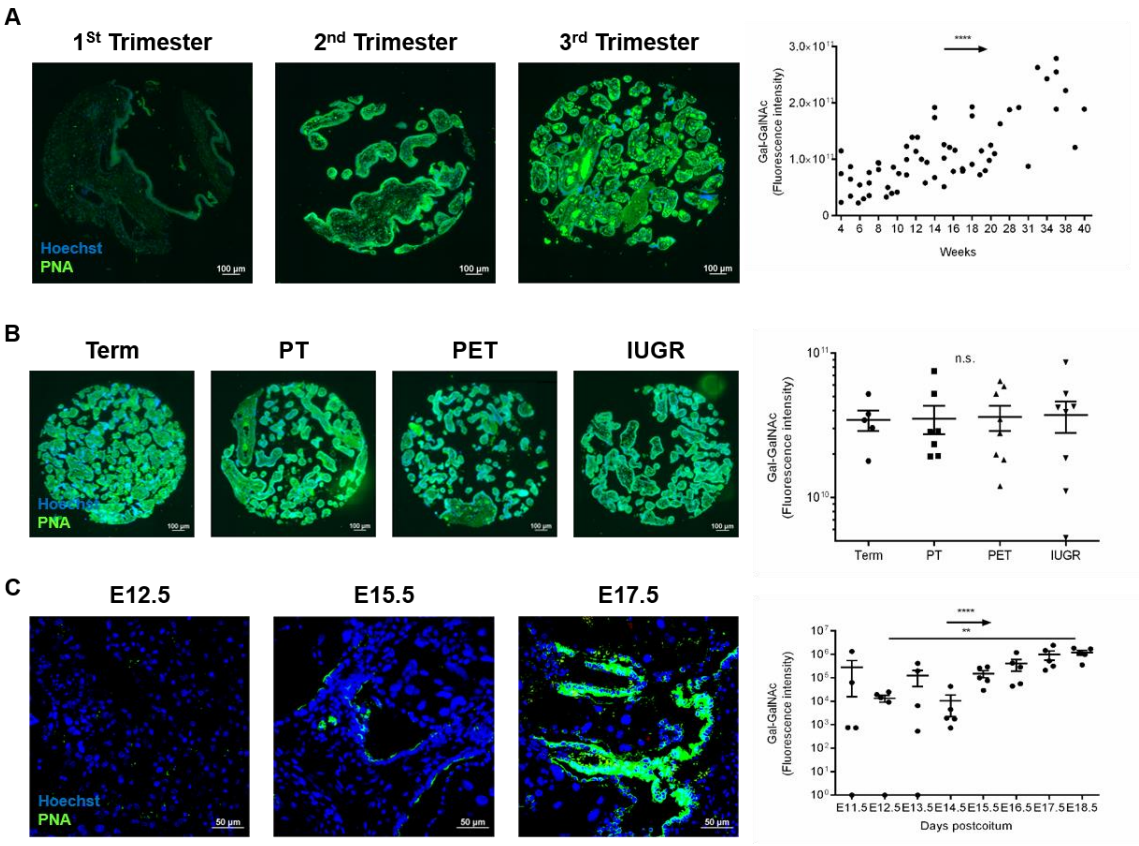

Figure 1. Gal-GalNAc level increases in human and mouse placenta along pregnancy progression. Human placenta TMA (TMA#2) was stained with FITC-labeled Gal-GalNAc-specific, PNA lectin (green) and Hoechst dye (blue).(A) Representative images of human placenta tissue of first, second and third trimester (left panels), and quantitative analysis of PNA binding (Sum of fluorescence intensity) to each TMA core (right panel). Each symbol represents the average of 2 replicate placental tissue cores per subject, n=63. Mean ± SEM are shown. ****$p < 0.0001$ represents the statistical significance of the increase in Gal-GalNAc levels along with placental ageing, using the Pearson correlation test. (B) Representative images of human placenta samples from term (Term, n=6), preterm (PT, n=6), Preeclampsia (PET, n=8), Intrauterine Growth Restriction (IUGR, n=8) pregnancies stained for Gal-GalNAc as described above (TMA#1) (left panels), and quantitative analysis of PNA binding (Sum of fluorescence intensity) to each TMA core (right panel). Each symbol represents the average of 4 replicate placental tissue cores per subject, Mean ± SEM are shown. n.s. = not significant two-tail Mann-Whitney test. (C) Representative images of mouse placenta tissue microarray cores stained with FITC-labeled Gal-GalNAc-specific PNA lectin (green) and Hoechst dye (blue) (left panel). Quantitative analysis of PNA binding (Sum of fluorescence intensity) to each TMA core (right panel, n=8 per day). Error bars indicate mean ± SEM. ****$p < 0.0001$ represents the statistical significance of the increase in Gal-GalNAc levels along with placental ageing, using the Pearson correlation test. **$p = 0.0079$, between E12 and E18.5 post gestation, two-tailed Mann-Whitney test. Data shown are representative of three independent reproducible experiments.

Figure 2

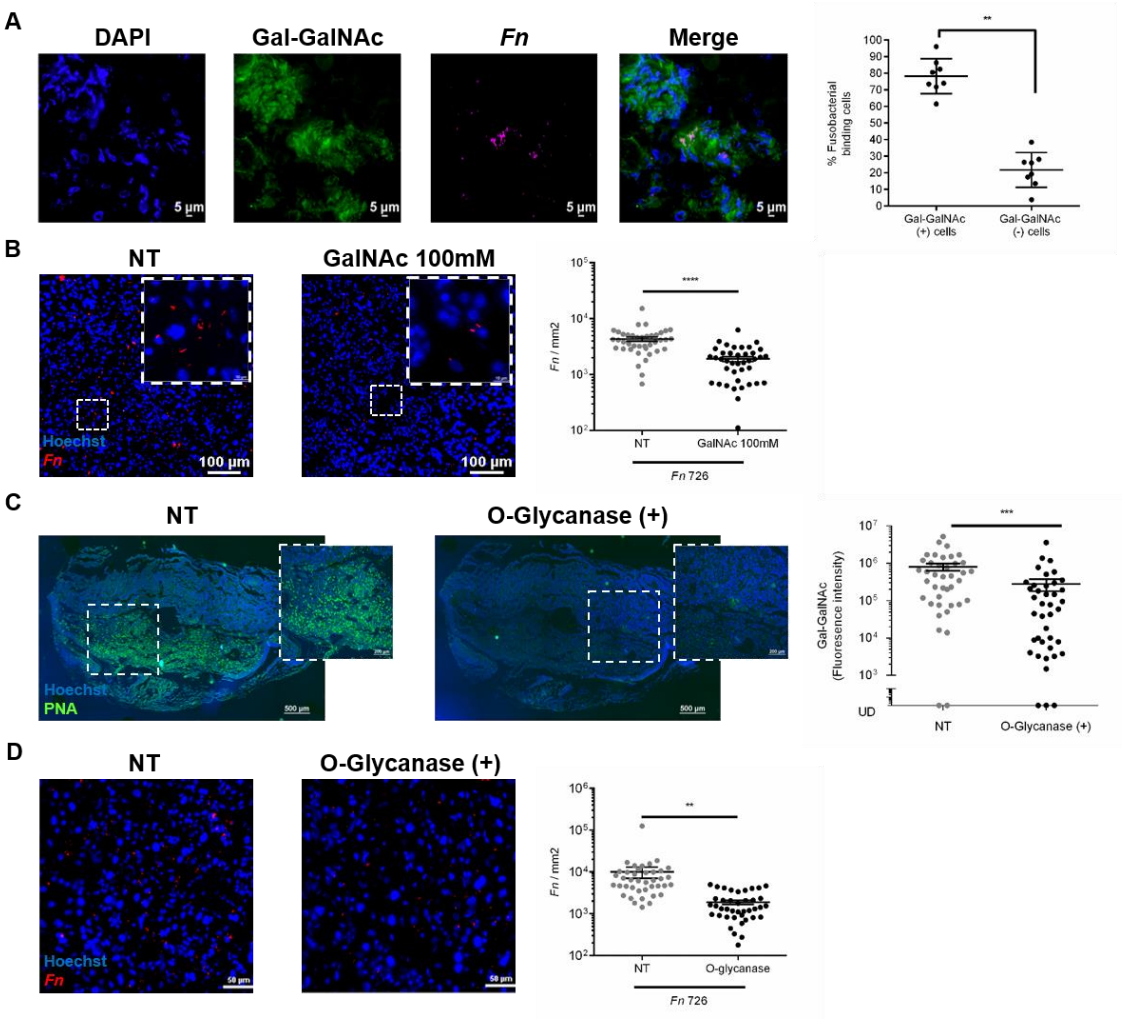

Figure 2. Gal-GalNAc mediates *F. nucleatum* attachment to mouse placenta. (A) Fusobacterial co-localization with Gal-GalNAc in mouse placenta. Representative image and quantitative analysis (% fusobacteria-binding cells) of Cy5-labeled (pink) *F. nucleatum* ATCC 23726 to mouse placental sections stained with Hoechst dye (blue), and FITC-labeled Gal-GalNAc-specific PNA lectin (green). Symbols represent individual cores each from a different mouse (n = 8). Mean ± SEM are shown; **p = 0.0039, one-tailed Wilcoxon signed-rank test. (B) Fusobacterial attachment to mouse placenta tissue is inhibited by Gal-GalNAc. Representative image (left panels) and quantitative analysis (*Fn*/mm^2) (right panel) of attachment of Cy3-labeled (red) *F. nucleatum* ATCC23726 to Hoechst-stained (blue) placental sections in the absence (not treated - NT), or presence (as indicated above) of 100 mM GalNAc. Magnification of the inset region are shown in the top-right corner. Each symbol represents the mean of two randomly selected fields per mouse TMA core, n=40. Error Mean ± SEM are shown. ****p < 0.0001, one-tailed Wilcoxon signed-rank test. (C) Removal of Gal-GalNAc in placenta sections using O-

glycanase. Representative images (left panels) and quantitative analysis (right panel) of mouse placenta TMA not treated (NT) or treated (as indicated) with O-glycanase and stained with Hoechst dye (blue), and FITC-labeled Gal-GalNAc-specific PNA lectin (green). Magnification of the inset are shown in the top-right corner. Symbols represent individual cores each from a different mouse, n=40. Mean ± SEM are shown. ***p = 0.0007, one-tailed Wilcoxon signed-rank test. (D) Fusobacterial Attachment to mouse placenta tissue is inhibited by Gal-GalNAc removal using O-glycanase. Representative images (left panels) and quantitative analysis (right panel) of attachment of Cy3-labeled (red) *F. nucleatum* ATCC 23726 to mouse placenta TMA untreated or treated (as indicated above) with O-glycanase, and stained with Hoechst dye (blue). Each symbol represents the mean of two randomly selected fields per mouse tissue core, n=40. Mean ± SEM are shown. **p = 0.0046, one-tailed Wilcoxon signed-rank test.

Figure 3

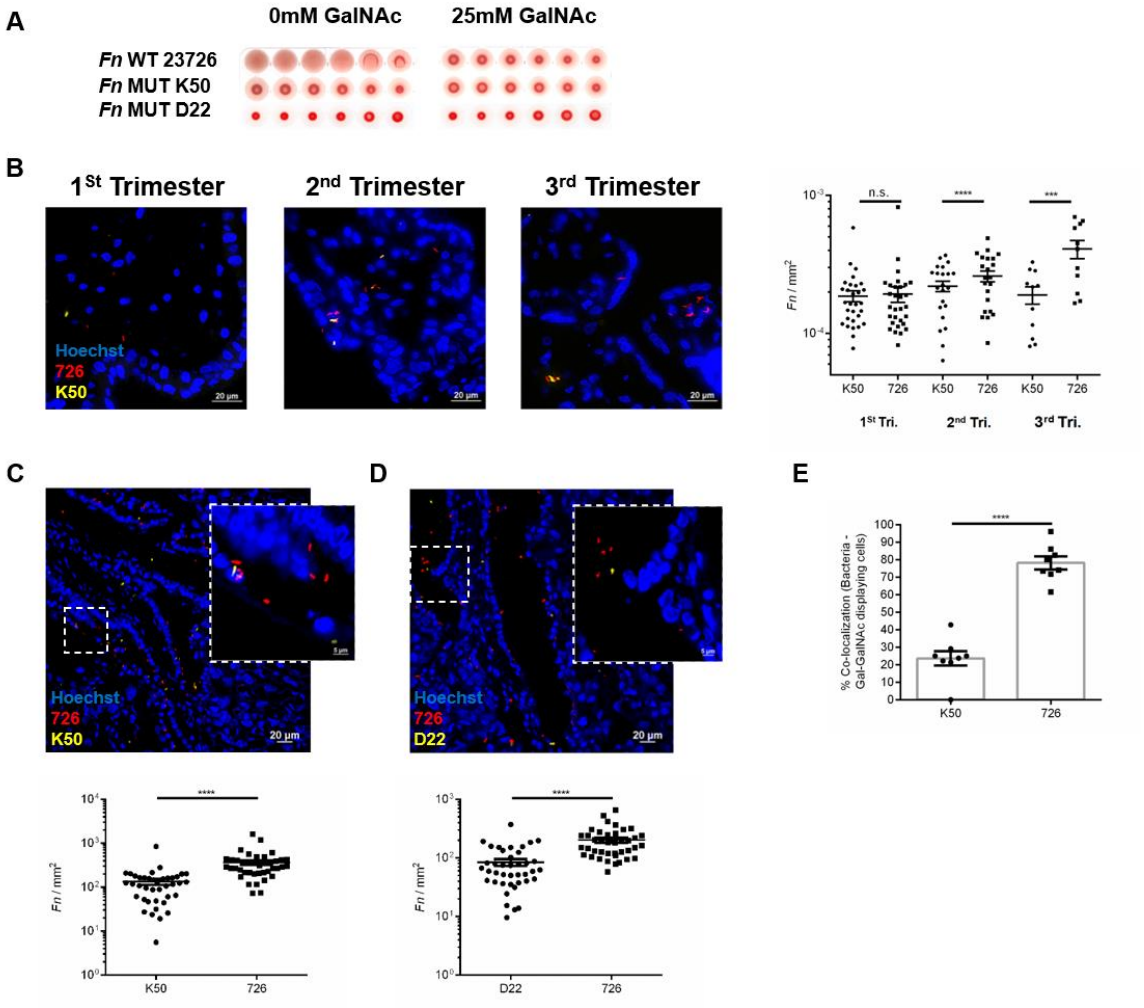

Figure 3. Fap2 mediates *F. nucleatum* attachment to human and mouse placenta. (A) Confirmation of Fap2 Gal-GalNAc binding activity by *F. nucleatum* ATCC 23726 (*Fn* WT 726) but not by its isogenic Fap2-inactivated mutants K50 and D22 by hemagglutination assay. Non-hemagglutinated erythrocytes settle in the bottom of the round bottom well. (B-D) Attachment of Cy3-labeled (red) *F. nucleatum* ATCC 23726 and of Cy5-labeled (yellow) Fap2-inactivated isogenic mutant K50 (B, C) or D22 (D) to Hoechst-stained (blue) representative human and mouse placenta sections respectively. Right panel in B and lower panels in C-D present quantitation of fusobacterial binding (*Fn*/mm^2) to human and mouse placenta samples. Magnification of the inset region in C and D are shown in the top-right corner. Each symbol represents the mean of two randomly selected fields per tissue core (average of 2 replicate placental tissue cores per subject in B), 1st trimester n=30, 2nd trimester n=22, 3rd trimester n=11 in B. n=40 in C and D. Mean ± SEM are shown; ****p < 0.0001, ***p = 0.0005, n.s = not significant, one-tailed Wilcoxon signed-rank test. (E) Co-localization analysis of *F. nucleatum* ATCC 23726 and of Fap2-inactivated isogenic mutant K50 with Gal-GalNAc displaying mouse placenta cells. Symbols represent

individual cores each from a different mouse (n = 8). Mean ± SEM are shown; ****p < 0.0001, one-tailed Wilcoxon signed-rank test.

Figure 4

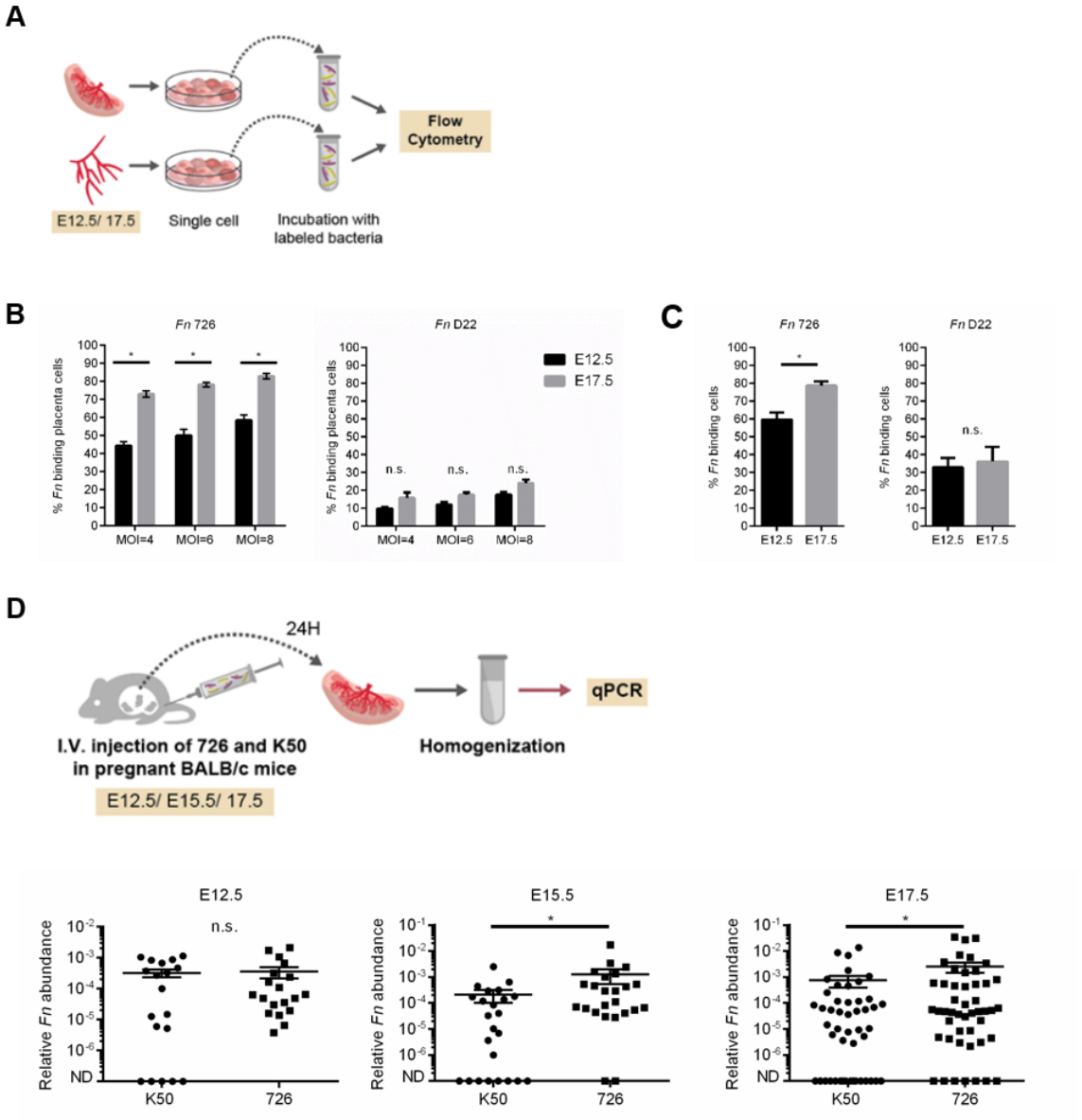

Figure 4. Gal-GalNAc - Fap2 mediated placenta attachment and colonization by *F. nucleatum* increases along pregnancy progression. (A) Experimental scheme: Blood vessels leading to the placenta and placentas were extracted from BALB/c mice at E12.5 and E17.5 of the pregnancy and single cells were prepared. The cells were incubated with FITC-labeled wild-type *Fn* ATCC 23726 and with the Fap2-inactivated isogenic mutant D22 labeled with Cy3. Bacterial attachment to the cells was analyze by flow cytometry. (B) Flow cytometry analyses of attachment (% binding cells) of FITC-labeled wild-type *Fn* ATCC 23726 and of Cy3-labeled D22 to cells extracted from mouse placenta at multiplicity of infection (MOI) of 4, 6 and 8 bacteria/cell. Mean values with SEM of

duplicate are shown. *p = 0.046, n.s. = not significant, one-tailed Mann-Whitney test. (C) Flow cytometry analyses of attachment (% binding cells) *Fn* ATCC 23726 and of Cy3-labeled D22 to cells extracted from mouse blood vessels leading to the placenta at multiplicity of infection (MOI) of 6 bacteria/cell. Mean values with SEM of duplicate are shown. *p = 0.046, n.s. = not significant, one-tailed Mann-Whitney test. (D) Experimental scheme: *Fn* WT 23726 were mixed with K50 (1 x 10^7 each) and inoculated iv to pregnant BALB/c mice at day E12.5, E15.5 or E17.5 of gestation. 24 hours later, mice were sacrificed, placentas harvested and fusobacteria quantified by qPCR (upper panel). Relative fusobacterial gDNA abundance ($2^{-\Delta Ct}$) of *Fn* WT 726 and of the Fap2-deficient isogenic mutant K50 in days of gestation: E12.5, E15.5 or E17.5. Each symbol represent a different placenta (lower panel). E12.5 n=5, E15.5 n=6, E17.5 n=12 (multiple placentas in each mouse). Mean ± SEM are shown; n.s.= not significant, *p = 0.0156 (E1.5), *p = 0.0317 (E17.5), one-tailed Wilcoxon signed-rank test. Data shown are representative of two independent reproducible experiments.

Figure 5

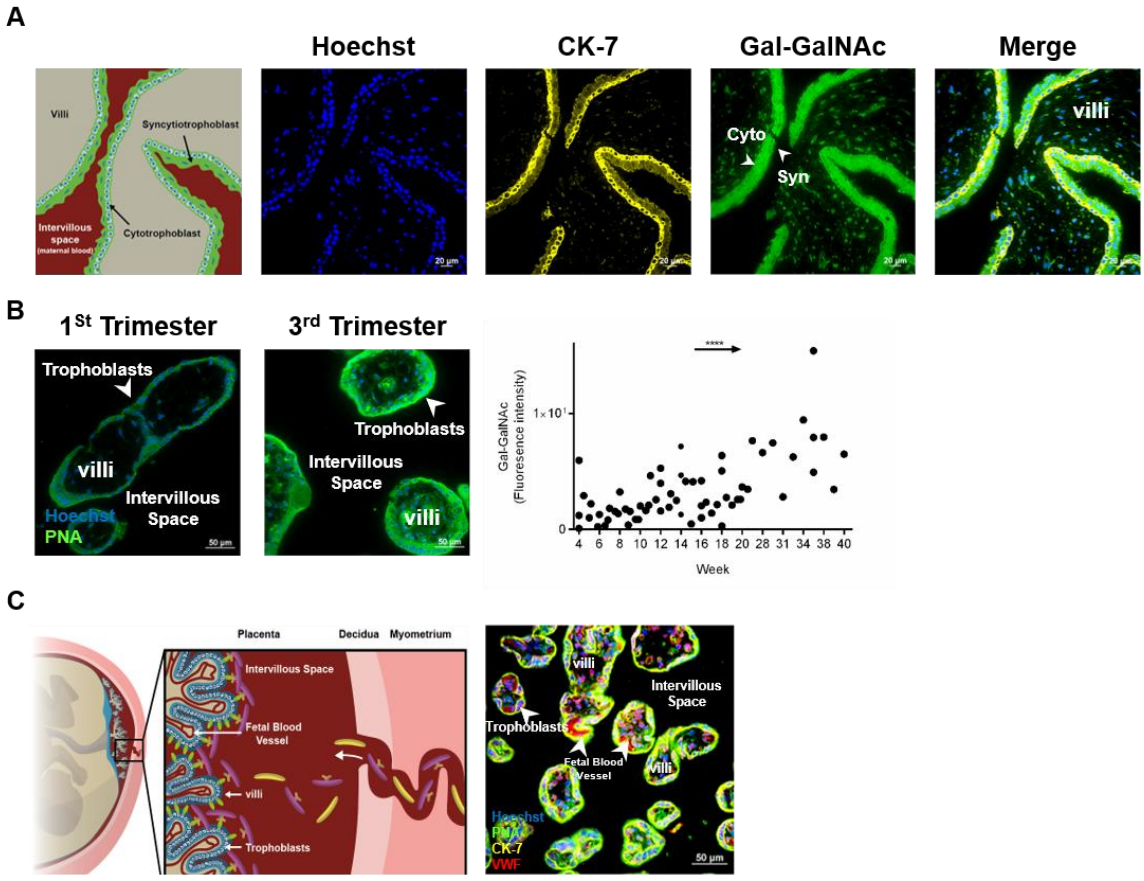

Figure 5. Gal-GalNAc is displayed to maternal blood in the intervillous space. (A-B) Representative images of human placenta TMA cores stained with FITC-labeled Gal-GalNAc-specific PNA lectin (green), Cy5-Cytokeratin-7 for trophoblasts cells (yellow) and Hoechst dye (blue). Quantitative analysis of PNA binding (Sum of fluorescence intensity) to each subject. Each symbol represents the average of 2 replicate cores, n=63. ****p < 0.0001. Gal-GalNAc increase in trophoblasts cells along pregnancy, Pearson correlation test (lower right panel). (C) Left panel shows a schematic model of human placenta colonization by *Fusobacterium nucleatum*. During transient bacteremia, bacteria enter the placenta with the maternal blood. Purple bacteria represent Fap2-expressing bacteria. Yellow bacteria represent bacteria lacking fap2. Gal-GalNAc the ligand for Fap2 binding, is represented with green stumps.

Right panel shows a human placenta section stained with FITC-labeled Gal-GalNAc-specific PNA lectin (green), Cy5-Cytokeratin-7 for trophoblasts cells (yellow), TRITC labeled Von Willebrand factor for identifying endothelial cells (red) and Hoechst dye (blue) (right panel). Syn – syncytiotrophoblasts, Cyt- cytotrophoblasts.

Figure 6

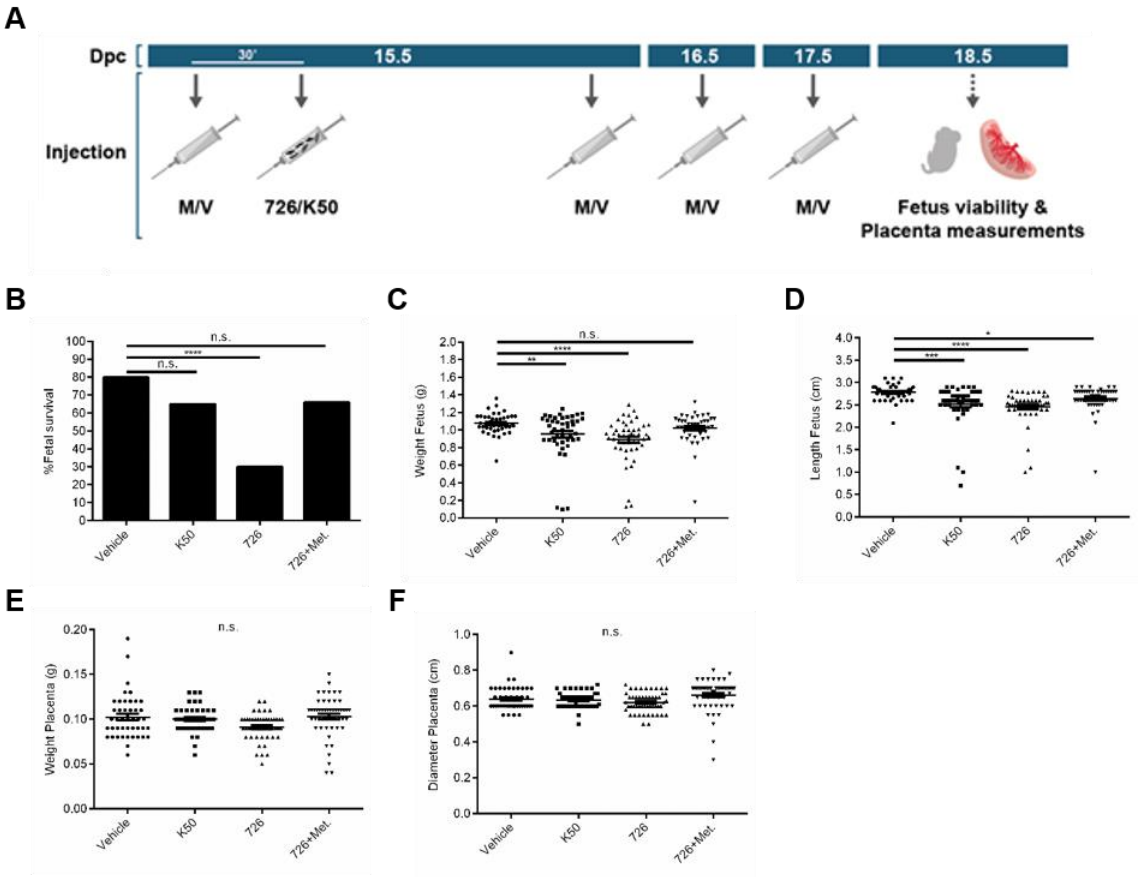

Figure 6. *F. nucleatum* 23726 cause fetal death that can be prevented with metronidazole. Experimental scheme: at day 15.5 of gestation BALB/c mice were sham IV inoculated with PBS vehicle, or IV inoculated with *F. nucleatum* ATCC 23726 or with K50. A sub-group of the mice inoculated with *F. nucleatum* ATCC 23726 were treated with metronidazole 30 minutes, 8h, 24h and 48h post inoculation. 72h post inoculation fetal viability and placenta parameters were measured. (B) Percent of fetal survival of the groups described in A. ****$p < 0.0001$, n.s. = not significant, one tailed Fisher's exact test for 2X2 tables. (C) Weight fetus indicated by gram. Error bars indicate mean ± SEM. ****$p < 0.0001$, one tailed, **$p = 0.0062$ two tailed, n.s. = not significant, T-test. (D) Length fetus indicated by cm. Error bars indicate mean ± SEM. ****$p < 0.0001$, one tailed, ***$p = 0.0009$, *$p = 0.0117$ one tailed, T-test. (E) Weight placenta indicated by gram. Error bars indicate mean ± SEM. n.s. = not significant, T-test. (F) Diameter placenta indicated by cm. Error bars indicate mean ± SEM. n.s. = not significant, T-test. Vehicle n = 44, K50 n = 46, 726 n = 50, 726+Met. n = 53.

STAR+METHODS

KEY RESOURCES TABLE

The key resources table is presented in an attached separate word document

LEAD CONTACT AND MATERIALS AVAILABILTY

Further information and requests for resources and reagents should be directed to and will be fulfilled by the Lead Contact, Gilad Bachrach (giladba@ekmd.huji.ac.il).

The mouse placenta Tissue Microarray created in this study is available upon request

DATA AND CODE AVAILABILITY

This study did not generate/analyze datasets/code.

EXPERIMENTAL MODEL AND SUBJECT DETAILS

In vivo animal studies

Timed pregnant BALB/cOlaHsd mice were purchased from Envigo (Israel). Mating was determined by the presence of a white vaginal plug. The day when the plug was detecte d was termed E0.5 of gestation. The pregnant mice were randomly assigned to experimental groups. All mouse experiments were carried out under protocol MD-17-15239-5 approved by the Hebrew University of Jerusalem Ethics Committee and signed by the chairman Prof. Sara Eyal. Mice were kept at a relative humidity 40–70%, 20–24 °C, and in 12 h dark/light cycles (07:00–19:00 light).

Human studies

The Hadassah Medical School institutional review board approved the use of human samples for this study. Human placenta tissue microarray TMA#1, TMA#2 array (RCWIH BioBank) were used in these studies. Details about the cases for each core on the array are available on the RCWIH BioBank Web site.

Bacterial strains

Bacterial strains used for probe validation are listed in the Key Resources Table. Bacteria were grown in Wilkins chalgren broth or on Columbia agar plates supplemented with 5% defibrinated sheep blood. The bacteria were grown in an anaerobic chamber in an atmosphere of 90% N2, 5% CO2 and 5% H2 at 37oC. Thiamphenicol (2.5 µg/ml) was added for mutant bacteria.

METHOD DETAILS

Hemagglutination Assays

Hemagglutination assays were performed as previously described (Coppenhagen-Glazer et al., 2015). For inhibition assays, washed bacteria were pre-incubated with 25mM GalNAc (Sigma-Aldrich) for 30 minutes prior to incubation with erythrocytes.

Tissue Microarray Analysis

Mouse placenta tissue microarray, containing mouse placenta tissue, punched from paraffin blocks along the pregnancy (E11.5 to E18.5)(Supplemental Figure) were constructed using the QuickRay® kit (UNITMA, Korea) according to the manufacturer's instructions. Human placenta tissue microarray TMA#1, TMA#2 array (RCWIH BioBank) were used in these studies.

Immunofluorescence and section preparation

TMA slides were stained with H&E or processed for immunofluorescence microscopy. TMA slides went through deparaffinization as follows: xylene twice 5 min, xylene 1 min, xylene/Ethanol (50%/50%) 1 min, ethanol twice 10 min, 90% ethanol 2 min, 80% ethanol 2 min, 70% ethanol 2 min and then washed in DDW. Slides went under heat-induced epitope retrieval using Sodium citrate 10 mM pH 6.0 in a microwave for 20 minutes, then 40 minutes in room temperature and wash 5 minutes in PBS. For PNA, anti-CK-7 and anti-von willebrand factor binding, sections were blocked with PBS supplemented with 10% BSA, 10% FBS, and 5% Triton for 2 h at room temperature followed by incubation with FITC labeled PNA (50 µg/ml in PBS), anti-CK-7 (1:200), or anti-von willebrand factor (1:500) overnight at 4 °C. The slides were then washed three times with PBS for 15 min and for anti-CK-7 and anti-von willebrand factor a second antibody Cy5 and Cy3 was added, respectively (Jackson, 1:100), for 2 h, washed three times with PBS for 15 min and then incubated with Hoechst 33258 diluted 1:5000 for 15 min at room temperature. Fluorescence intensity FITC-labeled PNA was evaluated using the ImagePro Analyzer 7.0 software. For fusobacterial binding, bacteria were labeled with Cy5 or Cy3 solution diluted 0.1 mg/ml in PBS. Sections were blocked with TBS (0.05 M Tris-HCl [pH 7.8], 0.1 M NaCl) supplemented with 20% BSA, 20% FBS and 5% Triton for 6h at room temperature, followed by incubation with the labeled bacteria (3×107 bacteria / ml blocking solution) for 6h at room temperature and then overnight at 4ºC. The slides were then washed once with PBS + TWEEN 0.5% followed by 2 washes with PBS for 15 min each, and then incubated with Hoechst 33258 diluted 1:5000 for 15 min at room temperature. GalNAc removal was performed by incubating sections with O-glycanase for 48 hours, washed for 5 minutes 3 timed with PBS prior to bacteria incubation. For competition bacteria was incubated with GalNAc (100 mM) for 30 min prior to incubation on the slide.

Flow cytometry

Timed pregnant BALB/cOlaHsd mice were purchased from Envigo. Mating was determined by the presence of a white vaginal plug. The day when the plug was detected was termed E0.5 of gestation. On E12.5 and E17.5 of gestation blood vessels leading to the placenta and placentas

were harvested, minced and treated with a collagenase type 4 (1 mg/ml) and DNase 1 (1 mg/ml) solution in PBS plus 1% fetal bovine serum (FBS) for 30 min at 37°C in a shaker bath. A total of 20 µl of 0.5 M EDTA per 2-ml sample was added to the digested tissues and incubated for an additional 15 min. The cells were washed, added 2 ml RBC Lysis Solution for 10 min washed again and filtered with a 70-µM filter.

FITC-labeled wild-type *Fn* ATCC 23726 and with the Fap2-inactivated isogenic mutant D22 labeled with Cy3 (MOI=4, 6, 8) were used for 30 min at 4ºC to the placentas cells and blood vessels leading to the placenta (MOI=6).

The stained samples were run in LSR II flow cytometers and further analyzed by Flowjo 10.0.8 software.

In vivo placental colonization-

Timed pregnant BALB/cOlaHsd mice were purchased, and mating was determined by the presence of a white vaginal plug. The day when the plug was detected was termed E0.5 of gestation. The pregnant mice were randomly distributed into study groups of 5 mice at E12.5, 6 mice at E15.5, 12 mice at E17.5. The pregnant mice were infected by ATCC 23726 wild type (WT) and the fap2 mutant K50 mixture by tail vein injection as follows. An aliquot of 100 µl of the bacterial suspension (5×107 CFU) or sterile PBS was injected into the tail vein. After 24 hours, the placentas were harvested from each pregnant mouse and homogenized under sterile conditions.

In vivo and antibiotic treatment-

Timed pregnant BALB/cOlaHsd mice at E15.5 were randomly distributed into four inoculation treatment groups: Sham inoculation with PBS; inoculation with *F. nucleatum* ATCC 23726; inoculation with *F. nucleatum* K50; with metronidazole or vehicle. We injected metronidazole or vehicle, after 30 minutes we injected bacteria and after 8 hours injected metronidazole or vehicle again. At E16.5 and E17.5 we injected metronidazole or vehicle and on E18.5 we harvested the placentas and checked fetus viability.

Quantification of bacteria using qPCR-

Placenta tissue samples were homogenized in 300 µl of PBS for 45 seconds at 4.5 m/s using a Fastprep and the DNA was extracted using the DNeasy Blood & Tissue Kit according to manufacturer's instructions. A custom TaqMan primer/probe set was used to amplify *F. nucleatum* DNA. The cycle threshold (Ct) values were normalized to the amount of murine gDNA in each reaction by using a primer/probe set for the reference gene (Gapdh). Each reaction contained 1 ng of DNA and was assayed in triplicate in 20 µL reactions containing 2× qPCRBIO

Lo-ROX Probe Mix as appropriate for individual qPCR machines. Reaction conditions were as follows: 2 min at 50 °C, 10 min at 95 °C, and 40 cycles of 15 s at 95 °C, and 1 min at 60 °C16. The sequences of all primers can be found in Supplementary Table 1.

QUANTIFICATION AND STATISTICAL ANALYSIS

Nonparametric Tests, IBM SPSS Statistics for Windows, Version 25, 2017, Armonk, NY: IBM Corp. and GraphPad Prism software version 6.0 was used for statistical analysis and presentation. Statistical tests used are indicated in the figure legends.

11.5	11.5	11.5	12.5	12.5
13.5	13.5	13.5	14.5	14.5
15.5	15.5	15.5	16.5	16.5
17.5	17.5	17.5	18.5	18.5

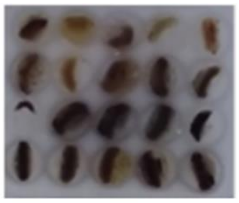

12.5	12.5	12.5	11.5	11.5
14.5	14.5	14.5	13.5	13.5
16.5	16.5	16.5	15.5	15.5
18.5	18.5	18.5	17.5	17.5

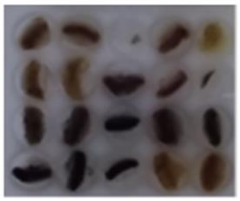

Supplementary Figure 1: Mouse tissue microarrays 1 and 2. The age of each placenta tissue is indicated in the table at the left of each array.

Supplementary Table 1

Primers used in this study

Name	Forward	Reveres	FAM Probe
F. nucleatum ATCC 237726 nusG	5'-CAACCATTACTTTAACTCTACC ATGTTCA 3'	5' ATTGACTTTACTGAGGGAGATTATG TA AAAATC 3'	5'- /56-FAM/TCAGCAACT/ZEN/TGTCCTTCTTGATCTTTA A ATGAACC/3IABkFQ/ -3'
F. nucleatum K50 catP	5'-GAAGGTTGACCACGGTATC AT3'	5'-CGCAACGGTATGGAAACAATC-3'	5'-/56-FAM/ATGGAAGGA/ZEN/AAGCCAAATGCTCCG /3IABkFQ/-3'
Mouse Gapdh	5'-AATGGTGAAGGTCGGTGTG -3'	5'-AATGGTGAAGGTCGGTGTG-3'	5'-/56-FAM/TGCAAATGG/ZEN/CAGCCCTGGTG/3IABkF Q/-3'

References

Aagaard, K., Ma, J., Antony, K.M., Ganu, R., Petrosino, J., and Versalovic, J. (2014). The placenta harbors a unique microbiome. Sci Transl Med *6*, 237ra265.

Aagaard, K.M. (2020). Mode of delivery and pondering potential sources of the neonatal microbiome. EBioMedicine *51*, 102554.

Abed, J., Emgard, J.E., Zamir, G., Faroja, M., Almogy, G., Grenov, A., Sol, A., Naor, R., Pikarsky, E., Atlan, K.A., *et al.* (2016). Fap2 Mediates *Fusobacterium nucleatum* Colorectal Adenocarcinoma Enrichment by Binding to Tumor-Expressed Gal-GalNAc. Cell Host Microbe *20*, 215-225.

Abed, J., Maalouf, N., Parhi, L., Chaushu, S., Mandelboim, O., and Bachrach, G. (2017). Tumor Targeting by Fusobacterium nucleatum: A Pilot Study and Future Perspectives. Front Cell Infect Microbiol *7*, 295.

Agerbaek, M.O., Bang-Christensen, S., and Salanti, A. (2019). Fighting Cancer Using an Oncofetal Glycosaminoglycan-Binding Protein from Malaria Parasites. Trends Parasitol *35*, 178-181.

Ayres Pereira, M., Mandel Clausen, T., Pehrson, C., Mao, Y., Resende, M., Daugaard, M., Riis Kristensen, A., Spliid, C., Mathiesen, L., L, E.K., *et al.* (2016). Placental Sequestration of *Plasmodium falciparum* Malaria Parasites Is Mediated by the Interaction Between VAR2CSA and Chondroitin Sulfate A on Syndecan-1. PLoS Pathog *12*, e1005831.

Bachrach, G., Ianculovici, C., Naor, R., and Weiss, E.I. (2005). Fluorescence based measurements of *Fusobacterium nucleatum* coaggregation and of fusobacterial attachment to mammalian cells. FEMS Microbiol Lett *248*, 235-240.

Barr, N., Taylor, C.R., Young, T., and Springer, G.F. (1989). Are pancarcinoma T and Tn differentiation antigens? Cancer *64*, 834-841.

Bobetsis, Y.A., Graziani, F., Gursoy, M., and Madianos, P.N. (2020). Periodontal disease and adverse pregnancy outcomes. Periodontol 2000 *83*, 154-174.

Coppenhagen-Glazer, S., Sol, A., Abed, J., Naor, R., Zhang, X., Han, Y.W., and Bachrach, G. (2015). Fap2 of *Fusobacterium nucleatum* is a galactose-inhibitable adhesin involved in coaggregation, cell adhesion, and preterm birth. Infect Immun *83*, 1104-1113.

Dayer, M.J., Jones, S., Prendergast, B., Baddour, L.M., Lockhart, P.B., and Thornhill, M.H. (2015). Incidence of infective endocarditis in England, 2000-13: a secular trend, interrupted time-series analysis. Lancet *385*, 1219-1228.

de Goffau, M.C., Lager, S., Sovio, U., Gaccioli, F., Cook, E., Peacock, S.J., Parkhill, J., Charnock-Jones, D.S., and Smith, G.C.S. (2019). Human placenta has no microbiome but can contain potential pathogens. Nature *572*, 329-334.

Dudley, D.J. (2020). The placental microbiome: yea, nay or maybe? BJOG *127*, 170.

El Costa, H., Tabiasco, J., Berrebi, A., Parant, O., Aguerre-Girr, M., Piccinni, M.P., and Le Bouteiller, P. (2009). Effector functions of human decidual NK cells in healthy early pregnancy are dependent on the specific engagement of natural cytotoxicity receptors. J Reprod Immunol *82*, 142-147.

Figuero, E., Han, Y.W., and Furuichi, Y. (2020). Periodontal diseases and adverse pregnancy outcomes: Mechanisms. Periodontol 2000 *83*, 175-188.

Gamliel, M., Goldman-Wohl, D., Isaacson, B., Gur, C., Stein, N., Yamin, R., Berger, M., Grunewald, M., Keshet, E., Rais, Y., *et al.* (2018). Trained Memory of Human Uterine NK Cells Enhances Their Function in Subsequent Pregnancies. Immunity *48*, 951-962 e955.

Goldenberg, R.L., Hauth, J.C., and Andrews, W.W. (2000). Intrauterine infection and preterm delivery. N Engl J Med *342*, 1500-1507.

Goldenberg, R.L., McClure, E.M., Saleem, S., and Reddy, U.M. (2010). Infection-related stillbirths. Lancet *375*, 1482-1490.

Gschwind, R., Fournier, T., Kennedy, S., Tsatsaris, V., Cordier, A.G., Barbut, F., Butel, M.J., and Wydau-Dematteis, S. (2020). Evidence for contamination as the origin for bacteria found in human placenta rather than a microbiota. PLoS One *15*, e0237232.

Gur, C., Ibrahim, Y., Isaacson, B., Yamin, R., Abed, J., Gamliel, M., Enk, J., Bar-On, Y., Stanietsky-Kaynan, N., Coppenhagen-Glazer, S.*, et al.* (2015). Binding of the Fap2 Protein of *Fusobacterium nucleatum* to Human Inhibitory Receptor TIGIT Protects Tumors from Immune Cell Attack. Immunity *42*, 344-355.

Gursoy, M., Gursoy, U.K., Sorsa, T., Pajukanta, R., and Kononen, E. (2013). High salivary estrogen and risk of developing pregnancy gingivitis. J Periodontol *84*, 1281-1289.

Han, Y.W., Fardini, Y., Chen, C., Iacampo, K.G., Peraino, V.A., Shamonki, J.M., and Redline, R.W. (2010). Term stillbirth caused by oral Fusobacterium nucleatum. Obstet Gynecol *115*, 442-445.

Han, Y.W., Redline, R.W., Li, M., Yin, L., Hill, G.B., and McCormick, T.S. (2004). *Fusobacterium nucleatum* induces premature and term stillbirths in pregnant mice: implication of oral bacteria in preterm birth. Infect Immun *72*, 2272-2279.

Han, Y.W., Shen, T., Chung, P., Buhimschi, I.A., and Buhimschi, C.S. (2009). Uncultivated bacteria as etiologic agents of intra-amniotic inflammation leading to preterm birth. J Clin Microbiol *47*, 38-47.

Han, Y.W., Shi, W., Huang, G.T., Kinder Haake, S., Park, N.H., Kuramitsu, H., and Genco, R.J. (2000). Interactions between periodontal bacteria and human oral epithelial cells: *Fusobacterium nucleatum* adheres to and invades epithelial cells. Infect Immun *68*, 3140-3146.

Hill, G.B. (1993). Investigating the source of amniotic fluid isolates of *fusobacteria*. Clin Infect Dis *16 Suppl 4*, S423-424.

Hill, G.B. (1998). Preterm birth: associations with genital and possibly oral microflora. Ann Periodontol *3*, 222-232.

Holtan, S.G., Creedon, D.J., Haluska, P., and Markovic, S.N. (2009). Cancer and pregnancy: parallels in growth, invasion, and immune modulation and implications for cancer therapeutic agents. Mayo Clin Proc *84*, 985-1000.

Ikegami, A., Chung, P., and Han, Y.W. (2009). Complementation of the fadA mutation in *Fusobacterium nucleatum* demonstrates that the surface-exposed adhesin promotes cellular invasion and placental colonization. Infect Immun *77*, 3075-3079.

Janitzek, C.M., Peabody, J., Thrane, S., P, H.R.C., T, G.T., Salanti, A., Chackerian, B., M, A.N., and Sander, A.F. (2019). A proof-of-concept study for the design of a VLP-based combinatorial HPV and placental malaria vaccine. Sci Rep *9*, 5260.

Jeschke, U., Mayr, D., Schiessl, B., Mylonas, I., Schulze, S., Kuhn, C., Friese, K., and Walzel, H. (2007). Expression of galectin-1, -3 (gal-1, gal-3) and the Thomsen-Friedenreich (TF) antigen in normal, IUGR, preeclamptic and HELLP placentas. Placenta *28*, 1165-1173.

Jeschke, U., Richter, D.U., Hammer, A., Briese, V., Friese, K., and Karsten, U. (2002). Expression of the Thomsen-Friedenreich antigen and of its putative carrier protein mucin 1 in the human placenta and in trophoblast cells in vitro. Histochem Cell Biol *117*, 219-226.

Kaplan, C.W., Lux, R., Huynh, T., Jewett, A., Shi, W., and Haake, S.K. (2005). Fusobacterium nucleatum apoptosis-inducing outer membrane protein. J Dent Res *84*, 700-704.

Kaplan, C.W., Ma, X., Paranjpe, A., Jewett, A., Lux, R., Kinder-Haake, S., and Shi, W. (2010). Fusobacterium nucleatum outer membrane proteins Fap2 and RadD induce cell death in human lymphocytes. Infect Immun *78*, 4773-4778.

Kolenbrander, P.E., and London, J. (1993). Adhere today, here tomorrow: oral bacterial adherence. J Bacteriol *175*, 3247-3252.

Koopman, L.A., Kopcow, H.D., Rybalov, B., Boyson, J.E., Orange, J.S., Schatz, F., Masch, R., Lockwood, C.J., Schachter, A.D., Park, P.J., *et al.* (2003). Human decidual natural killer cells are a unique NK cell subset with immunomodulatory potential. J Exp Med *198*, 1201-1212.

Liu, H., Redline, R.W., and Han, Y.W. (2007). *Fusobacterium nucleatum* induces fetal death in mice via stimulation of TLR4-mediated placental inflammatory response. J Immunol *179*, 2501-2508.

Liu, L., Johnson, H.L., Cousens, S., Perin, J., Scott, S., Lawn, J.E., Rudan, I., Campbell, H., Cibulskis, R., Li, M., *et al.* (2012). Global, regional, and national causes of child mortality: an updated systematic analysis for 2010 with time trends since 2000. Lancet *379*, 2151-2161.

Lockhart, P.B., Brennan, M.T., Sasser, H.C., Fox, P.C., Paster, B.J., and Bahrani-Mougeot, F.K. (2008). Bacteremia associated with toothbrushing and dental extraction. Circulation *117*, 3118-3125.

Loe, H., and Silness, J. (1963). Periodontal Disease in Pregnancy. I. Prevalence and Severity. Acta Odontol Scand *21*, 533-551.

Moore, W.E., and Moore, L.V. (1994). The bacteria of periodontal diseases. Periodontol 2000 *5*, 66-77.

Naeye, R.L., and Peters, E.C. (1978). Amniotic fluid infections with intact membranes leading to perinatal death: a prospective study. Pediatrics *61*, 171-177.

Nozawa, A., Oshima, H., Togawa, N., Nozaki, T., and Murakami, S. (2020). Development of Oral Care Chip, a novel device for quantitative detection of the oral microbiota associated with periodontal disease. PLoS One *15*, e0229485.

Offenbacher, S., Katz, V., Fertik, G., Collins, J., Boyd, D., Maynor, G., McKaig, R., and Beck, J. (1996). Periodontal infection as a possible risk factor for preterm low birth weight. J Periodontol *67*, 1103-1113.

Parhi, L., Alon-Maimon, T., Sol, A., Nejman, D., Shhadeh, A., Fainsod-Levi, T., Yajuk, O., Isaacson, B., Abed, J., Maalouf, N., *et al.* (2020). Breast cancer colonization by Fusobacterium nucleatum accelerates tumor growth and metastatic progression. Nat Commun *11*, 3259.

Richter, D.U., Jeschke, U., Makovitzky, J., Goletz, S., Karsten, U., Briese, V., and Friese, K. (2000). Expression of the Thomsen-Friedenreich (TF) antigen in the human placenta. Anticancer Res *20*, 5129-5133.

Salanti, A., Clausen, T.M., Agerbaek, M.O., Al Nakouzi, N., Dahlback, M., Oo, H.Z., Lee, S., Gustavsson, T., Rich, J.R., Hedberg, B.J., *et al.* (2015). Targeting Human Cancer by a Glycosaminoglycan Binding Malaria Protein. Cancer Cell *28*, 500-514.

Sanders, B.E., Umana, A., Lemkul, J.A., and Slade, D.J. (2018). FusoPortal: an Interactive Repository of Hybrid MinION-Sequenced Fusobacterium Genomes Improves Gene Identification and Characterization. mSphere *3*.

Seiler, R., Oo, H.Z., Tortora, D., Clausen, T.M., Wang, C.K., Kumar, G., Pereira, M.A., Orum-Madsen, M.S., Agerbaek, M.O., Gustavsson, T., *et al.* (2017). An Oncofetal Glycosaminoglycan Modification Provides Therapeutic Access to Cisplatin-resistant Bladder Cancer. Eur Urol *72*, 142-150.

Socransky, S.S., Haffajee, A.D., Cugini, M.A., Smith, C., and Kent, R.L., Jr. (1998). Microbial complexes in subgingival plaque. J Clin Periodontol *25*, 134-144.

Springer, G.F., Desai, P.R., and Banatwala, I. (1975). Blood group MN antigens and precursors in normal and malignant human breast glandular tissue. J Natl Cancer Inst *54*, 335-339.

Theis, K.R., Romero, R., Winters, A.D., Jobe, A.H., and Gomez-Lopez, N. (2020). Lack of Evidence for Microbiota in the Placental and Fetal Tissues of Rhesus Macaques. mSphere *5*.

Thornhill, M.H., Gibson, T.B., Cutler, E., Dayer, M.J., Chu, V.H., Lockhart, P.B., O'Gara, P.T., and Baddour, L.M. (2018). Antibiotic Prophylaxis and Incidence of Endocarditis Before and After the 2007 AHA Recommendations. J Am Coll Cardiol *72*, 2443-2454.

Vander Haar, E.L., So, J., Gyamfi-Bannerman, C., and Han, Y.W. (2018). *Fusobacterium nucleatum* and adverse pregnancy outcomes: Epidemiological and mechanistic evidence. Anaerobe *50*, 55-59.

Villamor-Martinez, E., Lubach, G.A., Rahim, O.M., Degraeuwe, P., Zimmermann, L.J., Kramer, B.W., and Villamor, E. (2020). Association of Histological and Clinical Chorioamnionitis With Neonatal Sepsis Among Preterm Infants: A Systematic Review, Meta-Analysis, and Meta-Regression. Front Immunol *11*, 972.

Wang, Y., and Zhao, S. (2010). In Vascular Biology of the Placenta (San Rafael (CA)).

Watts, D.H., Krohn, M.A., Hillier, S.L., and Eschenbach, D.A. (1992). The association of occult amniotic fluid infection with gestational age and neonatal outcome among women in preterm labor. Obstet Gynecol *79*, 351-357.

Weiss, E.I., Shaniztki, B., Dotan, M., Ganeshkumar, N., Kolenbrander, P.E., and Metzger, Z. (2000). Attachment of Fusobacterium nucleatum PK1594 to mammalian cells and its coaggregation with periodontopathogenic bacteria are mediated by the same galactose-binding adhesin. Oral Microbiol Immunol *15*, 371-377.

Wilson, W., Taubert, K.A., Gewitz, M., Lockhart, P.B., Baddour, L.M., Levison, M., Bolger, A., Cabell, C.H., Takahashi, M., Baltimore, R.S.*, et al.* (2008). Prevention of infective endocarditis: guidelines from the American Heart Association: a guideline from the American Heart Association Rheumatic Fever, Endocarditis and Kawasaki Disease Committee, Council on Cardiovascular Disease in the Young, and the Council on Clinical Cardiology, Council on Cardiovascular Surgery and Anesthesia, and the Quality of Care and Outcomes Research Interdisciplinary Working Group. J Am Dent Assoc *139 Suppl*, 3S-24S.

World-Health-Organization (2018). Preterm birth.

Yang, G.Y., and Shamsuddin, A.M. (1996). Gal-GalNAc: a biomarker of colon carcinogenesis. Histol Histopathol *11*, 801-806.

Zhou, Y., Fisher, S.J., Janatpour, M., Genbacev, O., Dejana, E., Wheelock, M., and Damsky, C.H. (1997). Human cytotrophoblasts adopt a vascular phenotype as they differentiate - A strategy for successful endovascular invasion? J Clin Invest *99*, 2139-2151.

KEY RESOURCES TABLE

The table highlights the genetically modified organisms and strains, cell lines, reagents, software, and source data **essential** to reproduce results presented in the manuscript. Depending on the nature of the study, this may include standard laboratory materials (i.e., food chow for metabolism studies), but the Table is **not** meant to be comprehensive list of all materials and resources used (e.g., essential chemicals such as SDS, sucrose, or standard culture media don't need to be listed in the Table). **Items in the Table must also be reported in the Method Details section within the context of their use.** The number of **primers and RNA sequences** that may be listed in the Table is restricted to no more than ten each. If there are more than ten primers or RNA sequences to report, please provide this information as a supplementary document and reference this file (e.g., See Table S1 for XX) in the Key Resources Table.

Please note that ALL references cited in the Key Resources Table must be included in the References list. Please report the information as follows:

- **REAGENT or RESOURCE:** Provide full descriptive name of the item so that it can be identified and linked with its description in the manuscript (e.g., provide version number for software, host source for antibody, strain name). In the Experimental Models section, please include all models used in the paper and describe each line/strain as: model organism: name used for strain/line in paper: genotype. (i.e., Mouse: OXTR$^{fl/fl}$: B6.129(SJL)-Oxtr$^{tm1.1Wsy/J}$). In the Biological Samples section, please list all samples obtained from commercial sources or biological repositories. Please note that software mentioned in the Methods Details or Data and Software Availability section needs to be also included in the table. See the sample Table at the end of this document for examples of how to report reagents.

- **SOURCE:** Report the company, manufacturer, or individual that provided the item or where the item can obtained (e.g., stock center or repository). For materials distributed by Addgene, please cite the article describing the plasmid and include "Addgene" as part of the identifier. If an item is from another lab, please include the name of the principal investigator and a citation if it has been previously published. If the material is being reported for the first time in the current paper, please indicate as "this paper." For software, please provide the company name if it is commercially available or cite the paper in which it has been initially described.

- **IDENTIFIER:** Include catalog numbers (entered in the column as "Cat#" followed by the number, e.g., Cat#3879S). Where available, please include unique entities such as RRIDs, Model Organism Database numbers, accession numbers, and PDB or CAS IDs. For antibodies, if applicable and available, please also include the lot number or clone identity. For software or data resources, please include the URL where the resource can be downloaded. Please ensure accuracy of the identifiers, as they are essential for generation of hyperlinks to external sources when available. Please see the Elsevier list of Data Repositories with automated bidirectional linking for details. When listing more than one identifier for the same item, use semicolons to separate them (e.g. Cat#3879S; RRID: AB_2255011). If an identifier is not available, please enter "N/A" in the column.
    - ***A NOTE ABOUT RRIDs:*** We highly recommend using RRIDs as the identifier (in particular for antibodies and organisms, but also for software tools and databases). For more details on how to obtain or generate an RRID for existing or newly generated resources, please visit the RII or search for RRIDs.

Please use the empty table that follows to organize the information in the sections defined by the subheading, skipping sections not relevant to your study. Please do not add subheadings. To add a row, place the cursor at the end of the row above where you would like to add the row, just outside the right border of the table. Then press the ENTER key to add the row. Please delete empty rows. Each entry must be on a separate row; do not list multiple items in a single table cell. Please see the sample table at the end of this document for examples of how reagents should be cited.

TABLE FOR AUTHOR TO COMPLETE

Please upload the completed table as a separate document. ***Please do not add subheadings to the Key Resources Table.*** *If you wish to make an entry that does not fall into one of the subheadings below, please contact your handling editor. (****NOTE:*** *For authors publishing in Current Biology, please note that references within the KRT should be in numbered style, rather than Harvard.)*

KEY RESOURCES TABLE

REAGENT or RESOURCE	SOURCE	IDENTIFIER
Antibodies		
Mouse monoclonal Anti-Cytokeratin 7	Abcam	Cat# ab9021; RRID: AB_306947
Polyclonal rabbit Anti-von Willebrand factor (VWF)	Dako	A0082 Cat# A0082, RRID:AB_2315602
Cy™5 AffiniPure Donkey Anti-Mouse IgG (H+L)	Jackson ImmunoResearch Labs	Cat# 715-175-150, RRID:AB_2340819
Cy3-AffiniPure Fab Fragment Donkey Anti-Rabbit IgG (H+L)	Jackson ImmunoResearch Labs	Cat# 711-167-003, RRID:AB_2340606
Bacterial and Virus Strains		
Fusobacterium nucleatum	ATCC	ATCC 23726
Fusobacterium nucleatum K50	Coppenhagen-Glazer,. et al. 2015	
Fusobacterium nucleatum D22	Coppenhagen-Glazer,. et al. 2015	
Biological Samples		
Chemicals, Peptides, and Recombinant Proteins		
Wilkins chalgren broth	Oxoid, UK	CM0643
Columbia agar plates	Oxoid, UK	CM0331
Sheep blood	Novamed LTD, Israel	118289
Metronidazole 0.5mg\ml	B. Braun, Germany	
GalNAc	Sigma-Aldrich	A2795; CAS 1811-31-0
O-glycanase	Sigma-Aldrich	G1163; CAS 9032-92-2
Collagenase, Type 4	Worthington Biochemicals	LS004188
DNase 1	Roche	10104159001
EDTA	Biological Industries	01-862-1B
RBC Lysis Solution	Biological Industries	01-888-1B
Critical Commercial Assays		
DNeasy Blood & Tissue Kit	Qiagen, Germany	69506

Deposited Data		
Experimental Models: Cell Lines		
Experimental Models: Organisms/Strains		
BALB/cOlaHsd female mice	Envigo	
Oligonucleotides		
Primers, see Table S1	This paper	N/A
Recombinant DNA		
Software and Algorithms		
ImagePro Analyzer 7.0 software	Cybernetics, USA	
LSR II	BD Biosciences	
Flowjo 10.0.8 software	Tree Star, Ashland, OR, USA	
Other		
Hoechst 33258 solution	Sigma-Aldrich	94403; CAS 23491-45-4
Cy3 mono-Reactive Dye Pack,	Life sciences GE	PA23001
Cy5 mono-Reactive Dye Pack,	Life sciences GE	PA25001
Anaerobic chamber	Bactron I-II Shellab, USA	
QuickRay® kit	UNITMA, Korea	
Fastprep	MP Biomedicals, USA	
FITC-labeled PNA	Sigma-Aldrich	L7381
qPCRBIO Probe Mix Hi-Rox	PCRBiosystems	PB20.22-05

I'm not sure if I should add this to the table

Xylene	Gadot-group	P160070257; CAS 1330-20-7
Ethanol	Gadot-group	P190004867; CAS 64-17-5
Sodium citrate	J.T.Baker	3646-01; CAS 6132-04-3
PBS	Biological Industries	02-020-1A
BSA	Sigma-Aldrich	A7906; CAS 9048-46-8
FBS	Biological Industries	04-127-1A
Triton	J.T.Baker	X198-05; CAS 9002-93-1
TWEEN	J.T.Baker	X251-07; CAS 9005-64-5

TABLE WITH EXAMPLES FOR AUTHOR REFERENCE

REAGENT or RESOURCE	SOURCE	IDENTIFIER
Antibodies		
Rabbit monoclonal anti-Snail	Cell Signaling Technology	Cat#3879S; RRID: AB_2255011
Mouse monoclonal anti-Tubulin (clone DM1A)	Sigma-Aldrich	Cat#T9026; RRID: AB_477593
Rabbit polyclonal anti-BMAL1	This paper	N/A
Bacterial and Virus Strains		
pAAV-hSyn-DIO-hM3D(Gq)-mCherry	Krashes et al., 2011	Addgene AAV5; 44361-AAV5
AAV5-EF1a-DIO-hChR2(H134R)-EYFP	Hope Center Viral Vectors Core	N/A
Cowpox virus Brighton Red	BEI Resources	NR-88
Zika-SMGC-1, GENBANK: KX266255	Isolated from patient (Wang et al., 2016)	N/A
Staphylococcus aureus	ATCC	ATCC 29213
Streptococcus pyogenes: M1 serotype strain: strain SF370; M1 GAS	ATCC	ATCC 700294
Biological Samples		
Healthy adult BA9 brain tissue	University of Maryland Brain & Tissue Bank; http://medschool.umaryland.edu/btbank/	Cat#UMB1455
Human hippocampal brain blocks	New York Brain Bank	http://nybb.hs.columbia.edu/
Patient-derived xenografts (PDX)	Children's Oncology Group Cell Culture and Xenograft Repository	http://cogcell.org/
Chemicals, Peptides, and Recombinant Proteins		
MK-2206 AKT inhibitor	Selleck Chemicals	S1078; CAS: 1032350-13-2
SB-505124	Sigma-Aldrich	S4696; CAS: 694433-59-5 (free base)
Picrotoxin	Sigma-Aldrich	P1675; CAS: 124-87-8
Human TGF-β	R&D	240-B; GenPept: P01137
Activated S6K1	Millipore	Cat#14-486
GST-BMAL1	Novus	Cat#H00000406-P01
Critical Commercial Assays		
EasyTag EXPRESS 35S Protein Labeling Kit	Perkin-Elmer	NEG772014MC
CaspaseGlo 3/7	Promega	G8090
TruSeq ChIP Sample Prep Kit	Illumina	IP-202-1012
Deposited Data		
Raw and analyzed data	This paper	GEO: GSE63473
B-RAF RBD (apo) structure	This paper	PDB: 5J17

Human reference genome NCBI build 37, GRCh37	Genome Reference Consortium	http://www.ncbi.nlm.nih.gov/projects/genome/assembly/grc/human/
Nanog STILT inference	This paper; Mendeley Data	http://dx.doi.org/10.17632/wx6s4mj7s8.2
Affinity-based mass spectrometry performed with 57 genes	This paper; and Mendeley Data	Table S8; http://dx.doi.org/10.17632/5hvpvspw82.1
Experimental Models: Cell Lines		
Hamster: CHO cells	ATCC	CRL-11268
D. melanogaster: Cell line S2: S2-DRSC	Laboratory of Norbert Perrimon	FlyBase: FBtc0000181
Human: Passage 40 H9 ES cells	MSKCC stem cell core facility	N/A
Human: HUES 8 hESC line (NIH approval number NIHhESC-09-0021)	HSCI iPS Core	hES Cell Line: HUES-8
Experimental Models: Organisms/Strains		
C. elegans: Strain BC4011: srl-1(s2500) II; dpy-18(e364) III; unc-46(e177)rol-3(s1040) V.	Caenorhabditis Genetics Center	WB Strain: BC4011; WormBase: WBVar00241916
D. melanogaster: RNAi of Sxl: y[1] sc[*] v[1]; P{TRiP.HMS00609}attP2	Bloomington Drosophila Stock Center	BDSC:34393; FlyBase: FBtp0064874
S. cerevisiae: Strain background: W303	ATCC	ATTC: 208353
Mouse: R6/2: B6CBA-Tg(HDexon1)62Gpb/3J	The Jackson Laboratory	JAX: 006494
Mouse: OXTRfl/fl: B6.129(SJL)-Oxtr$^{tm1.1Wsy}$/J	The Jackson Laboratory	RRID: IMSR_JAX:008471
Zebrafish: Tg(Shha:GFP)t10: t10Tg	Neumann and Nuesslein-Volhard, 2000	ZFIN: ZDB-GENO-060207-1
Arabidopsis: 35S::PIF4-YFP, BZR1-CFP	Wang et al., 2012	N/A
Arabidopsis: JYB1021.2: pS24(AT5G58010)::cS24:GFP(-G):NOS #1	NASC	NASC ID: N70450
Oligonucleotides		
siRNA targeting sequence: PIP5K I alpha #1: ACACAGUACUCAGUUGAUA	This paper	N/A
Primers for XX, see Table SX	This paper	N/A
Primer: GFP/YFP/CFP Forward: GCACGACTTCTTCAAGTCCGCCATGCC	This paper	N/A
Morpholino: MO-pax2a GGTCTGCTTTGCAGTGAATATCCAT	Gene Tools	ZFIN: ZDB-MRPHLNO-061106-5
ACTB (hs01060665_g1)	Life Technologies	Cat#4331182
RNA sequence: hnRNPA1_ligand: UAGGGACUUAGGGUUCUCUCUAGGGACUUAGGGUUCUCUCUAGGGA	This paper	N/A
Recombinant DNA		
pLVX-Tight-Puro (TetOn)	Clonetech	Cat#632162
Plasmid: GFP-Nito	This paper	N/A

cDNA GH111110	Drosophila Genomics Resource Center	DGRC:5666; FlyBase:FBcl0130415
AAV2/1-hsyn-GCaMP6- WPRE	Chen et al., 2013	N/A
Mouse raptor: pLKO mouse shRNA 1 raptor	Thoreen et al., 2009	Addgene Plasmid #21339
Software and Algorithms		
ImageJ	Schneider et al., 2012	https://imagej.nih.gov/ij/
Bowtie2	Langmead and Salzberg, 2012	http://bowtie-bio.sourceforge.net/bowtie2/index.shtml
Samtools	Li et al., 2009	http://samtools.sourceforge.net/
Weighted Maximal Information Component Analysis v0.9	Rau et al., 2013	https://github.com/ChristophRau/wMICA
ICS algorithm	This paper; Mendeley Data	http://dx.doi.org/10.17632/5hvpvspw82.1
Other		
Sequence data, analyses, and resources related to the ultra-deep sequencing of the AML31 tumor, relapse, and matched normal.	This paper	http://aml31.genome.wustl.edu
Resource website for the AML31 publication	This paper	https://github.com/chrisamiller/aml31SuppSite